

HIGH-FIDELITY AEROELASTIC ANALYSIS OF PASSIVE FOLDING-WING CONCEPTS FOR GUST LOAD MITIGATION: COUPLED CFD/CSD COMPUTATIONAL STUDY

Majid Ahmadi, Turaç Farsadi, Hüseyin Can Önel, Altan Kayran
and Hamed Haddad Khodaparast*

**Adana Science and Technology University,
Balcalı Mh. Güney Kampüs 10 Sk. No:1U, Sarıcam, Adana
Turkey*

ABSTRACT

This study presents a numerical framework for the design and analysis of a high aspect ratio composite wing equipped with a passive Folding WingTip (FWT) device aimed at gust load alleviation. A coupled fluid-structure interaction (FSI) simulation is employed, integrating ANSYS Mechanical for structural analysis and ANSYS Fluent for aerodynamic computations. The composite baseline wing, optimized in previous studies for minimum weight under structural and aeroelastic constraints, serves as the reference configuration. The passive FWT concept is incorporated at the wing tip to passively adapt to gust-induced aerodynamic loads without active control. The effectiveness of the passive folding mechanism is evaluated by examining reductions in the root bending moment under 1-cosine and harmonic gust excitations. Comparative analyses are conducted between the baseline wing and the wing equipped with the FWT, highlighting the potential of passive morphing concepts to enhance aeroelastic performance and passenger comfort by mitigating gust loads without adding significant complexity or weight to the wing system.

INTRODUCTION

High aspect ratio wings, while offering superior aerodynamic efficiency [1], are particularly susceptible to gust-induced loads due to their inherent flexibility [2, 3]. Gust events can generate significant unsteady aerodynamic forces, resulting in large Root Bending Moments (RBM) that threaten both the structural integrity and operational safety of the wing [4, 5]. Traditional fixed-wing designs lack mechanisms to adapt dynamically to these disturbances, leading to increased structural weight through conservative design margins [6, 7].

To address this challenge, passive morphing concepts such as Folding WingTip (FWT) devices have been introduced [8, 9]. Fig. 1 illustrates the meshed model of a composite wing equipped with a passive folding wingtip device, designed for numerical investigation [8, 10]. In this configuration, the outboard section of the wing is allowed to fold upward passively in response to aerodynamic loading, thereby reducing the effective lifting area during gust encounters and mitigating the peak load transmitted to the wing root [11, 12].

This study aims to perform a detailed fluid-structure interaction (FSI) analysis using a coupled Ansys Mechanical and Fluent framework to evaluate the effectiveness of the folding wingtip design. The main objective is to quantify the reduction in RBM and assess the aerodynamic-structural performance improvements achieved by the passive folding mechanism under gust loading conditions.

METHODOLOGY

Flow Solution (CFD)

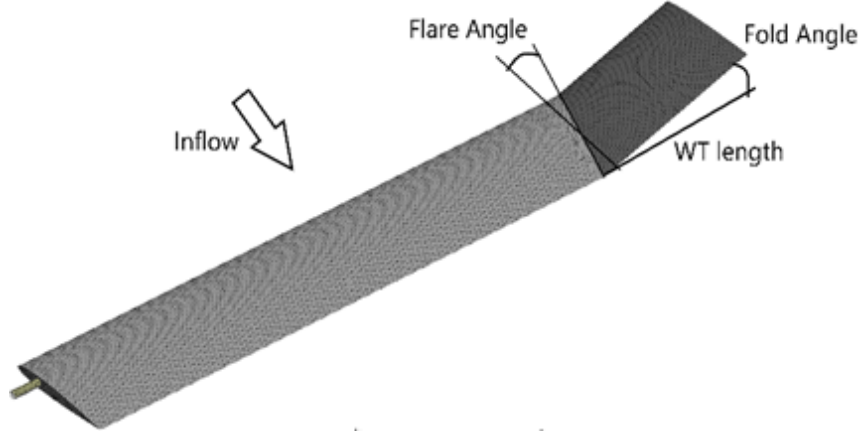


Figure 1: Schematic description of the folding wingtip showing key parameters: flare angle, fold angle, and wingtip (WT) length, with respect to the freestream inflow direction.

The fluid flow is simulated using the Ansys Fluent flow solver. The fluid is modeled as air, having a density of $\rho = 1.225 \text{ kg/m}^3$. As the angle of attack remains about $\alpha = 2.5^\circ$, flow adverse pressure effects are expected minimal to none over the NACA-0018 profile and the flow highly streamlined. Since drag plays a negligible role in this case, the flow is assumed inviscid to save computational resources and it yields reasonable lift values which is the prominent aerodynamic force in this case. Moreover, the freestream velocity is kept around $U_\infty = 20 \text{ m/s}$, which translates to very low compressibility with $M_\infty \approx 0.06$ at sea level conditions. With the addition of incompressibility, the Navier-Stokes equations reduces to Eq. (1) and Eq. (2) as Fluents handles them, which represent the conservation of mass and momentum, respectively.

$$\frac{\partial u_i}{\partial x_i} = 0 \quad (1)$$

$$\frac{\partial u_i}{\partial t} + u_j \frac{\partial u_i}{\partial x_j} = -\frac{1}{\rho} \frac{\partial p}{\partial x_i} \quad (2)$$

Here, the i and j indices denote the spatial coordinates in 3D space, and p is the static pressure. Second order schemes are used in both space and time, with 20 iterations at each timestep and 1×10^{-4} convergence criteria.

The solution grid consists of 1.96 million cells Fig. 2. Inlet and lateral boundaries are located 15c (chord) away from the wing in all directions to prevent boundary condition influence on the wing surface, and the outlet boundary lies 35c downstream. The wing root is located at $y=0$, where the domain boundary is defined as a symmetry plane along with the other lateral domain boundaries. Flow is driven with Dirichlet-type velocity inlet and pressure outlet boundary conditions in the $+x$ direction. Slip condition is applied at the wing surfaces, and coarse inflation layers are generated to obtain a better pressure distribution.

Structural Solution (CSD)

The process of modeling the wing in ANSYS begins with the creation of a detailed CAD model of the main wing and wingtip, ensuring that pivot points and hinges are accurately defined. This model is subsequently imported into ANSYS Design Modeler, where appropriate material properties are assigned to the components. In ANSYS Workbench, a revolute joint with specified torsional stiffness is defined under the “connections” module between the main wing and the wingtip. The rotational degree of freedom and the torsional stiffness of the joint

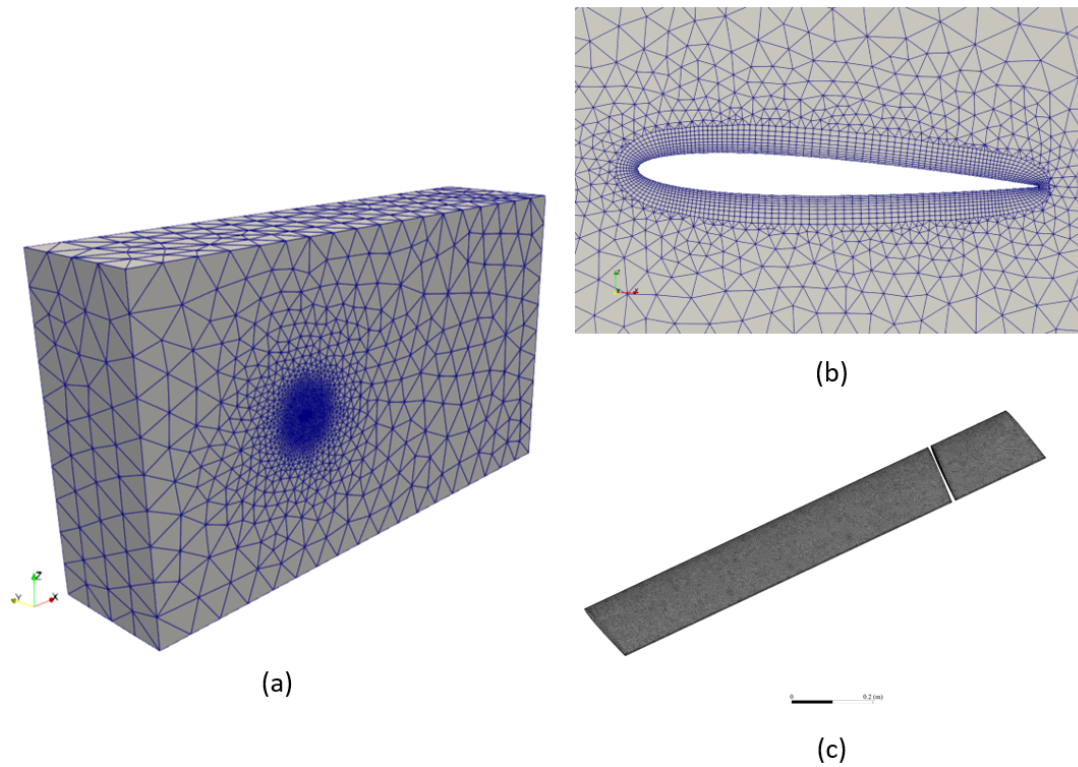


Figure 2: (a) The complete CFD domain, (b) Inflation layers around the wing surface, (c) Wing surface mesh within the CFD solution

are carefully specified. During the translation to APDL, it is crucial to ensure that this joint is represented by an MPC184 element. The MPC184 element effectively models the revolute joint with the defined torsional stiffness, accurately simulating the spring mechanism's behavior in the folding process. This configuration allows the wingtip to fold/twist under aerodynamic gust loads while providing resistance through the torsional spring.

Fluid-Structure Interaction (FSI) and Coupling

The two-way fluid-structure interaction (FSI) simulation is performed using a partitioned approach within ANSYS System Coupling, where the fluid and structural fields are solved by ANSYS Fluent and ANSYS Mechanical, respectively. The coupling interface is defined at the common fluid-structure boundary, and the solvers exchange data at each coupling iteration to satisfy interface conditions of kinematic compatibility and dynamic equilibrium (Fig. 3). At the interface, Fluent computes the aerodynamic loads, including pressure and shear forces, and transfers them to the structural solver as surface tractions. ANSYS Mechanical computes the structural response and returns the resulting displacements to Fluent. These displacements are used to deform the fluid mesh using dynamic mesh motion techniques, such as spring-based or diffusion-based smoothing, to maintain mesh quality during deformation.

Since the fluid and structural meshes are generally non-conforming, the data transfer is handled by profile-based interpolation and projection algorithms. The mapping is conservative: forces are distributed from fluid faces to structural nodes such that the total transferred force and moment are preserved, and structural displacements are interpolated back to the fluid surface nodes. This ensures that the interface exchange satisfies global equilibrium while maintaining local consistency. The coupling follows an implicit staggered scheme at each physical time step. Within each step, multiple coupling iterations are performed until both displacement and force

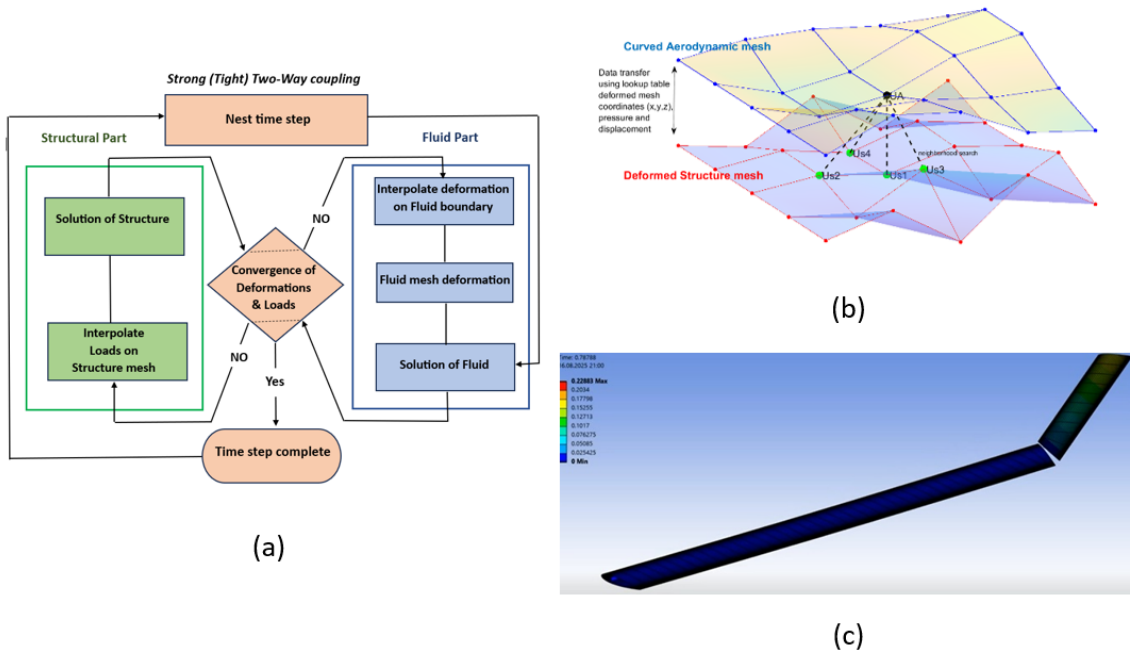


Figure 3: (a) Two-Way Coupling Method, (b) Data Transfer Between Structural and Fluid Meshes, (c) FSI Analysis of the Folding Wing

residuals fall below specified tolerances. For transient analysis, this procedure is repeated at every time increment, ensuring synchronized time advancement of both solvers. The objective of the coupled FSI simulations is to quantify the reduction in root bending moment (RBM) under gust excitation and to assess the feasibility of the passive FWT mechanism as an effective gust load alleviation strategy. Additionally, this methodology supports the optimization of wingtip geometry and hinge placement for improved aerodynamic performance and structural resilience. The outcomes of this analysis contribute to the broader goal of developing lighter, more efficient, and structurally safe wing configurations suitable for next-generation aircraft and UAV platforms.

RESULTS AND DISCUSSION

AGARD 445.6 wing, a widely used benchmark for aeroelastic validation, is employed here to validate the implemented static aeroelastic framework. In this work, we develop a model of the wing using published geometry and material data, and solve the coupled fluid structure interaction by iterating between an Euler based CFD solution in ANSYS Fluent and a structural solution in ANSYS Mechanical via System Coupling until convergence. The predicted aerodynamic coefficients and spanwise pressure distributions are consistent with prior literature and available experimental trends (Fig. 4 and Fig. 5). The computed tip deflection is also in close agreement with reported measurements. Overall discrepancies remain within the range commonly reported for this benchmark, attributable primarily to discretizations and solver setup effects, and the results confirm the suitability of the present framework for subsequent parametric and gust load studies.

Fig. 6 illustrates the hinge rotation (fold angle) and the vertical deflection of the base wing measured at the hinge location and at the leading edge. These responses clearly capture the coupled dynamic behaviour of the base wing and wingtip, providing direct insight into their interaction and its influence on the root bending moment (RBM).

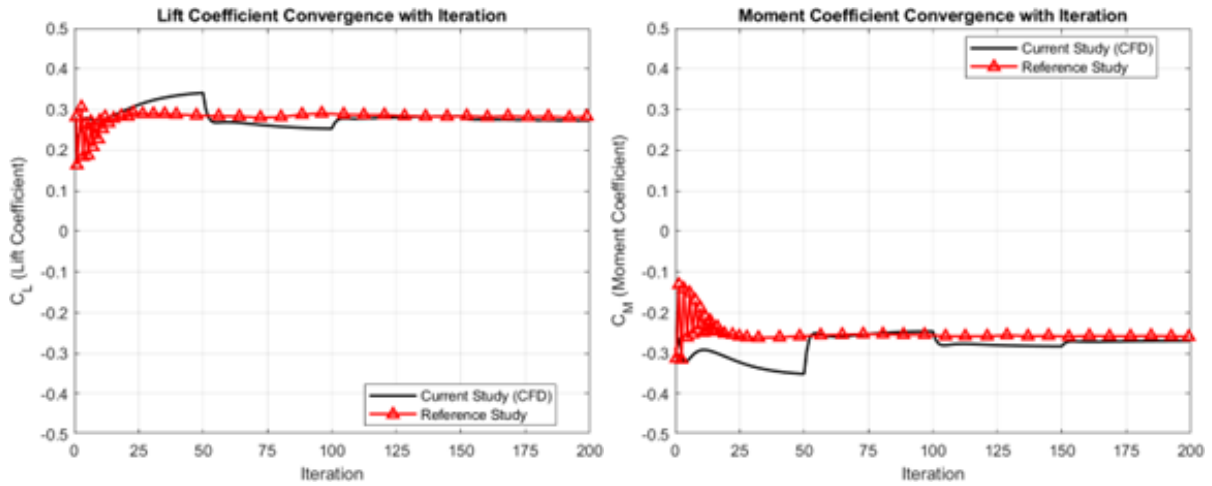


Figure 4: History of Lift Coefficient and Moment Coefficient for Elastic AGARD 445.6 Wing

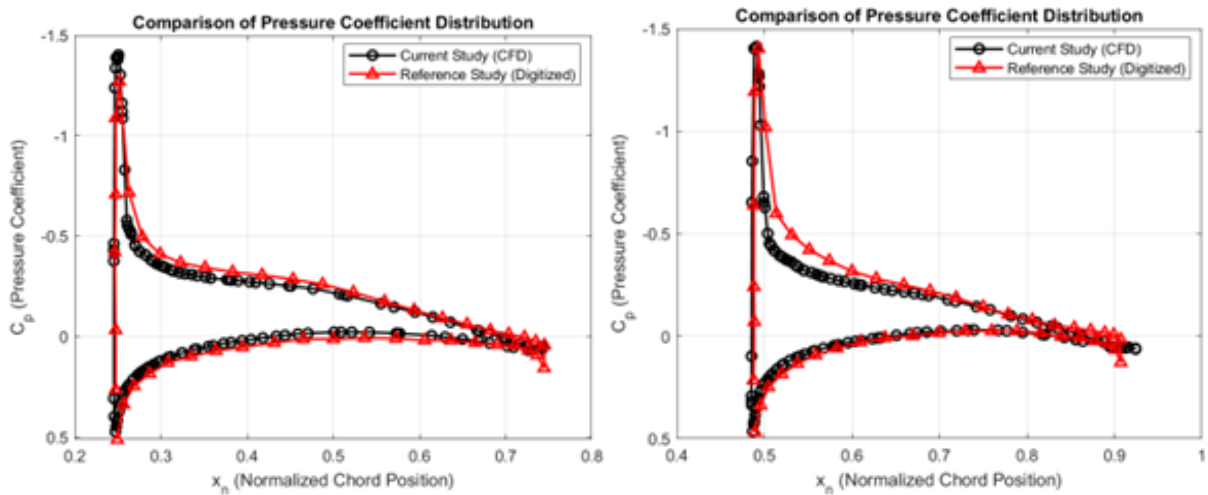


Figure 5: Comparison of the Pressure Distribution on 34% of the span, and the 67% of the span

Fig. 7 compares the positive and negative peak values at different gust frequencies. The results reveal that the RBM peaks in the positive direction, associated with downward wingtip rotation, are lower than those in the negative direction, corresponding to upward wingtip rotation. Furthermore, as the gust frequency increases at a constant gust ratio, the negative RBM peaks exhibit a continuous growth, whereas the positive peaks initially increase up to a gust frequency of approximately 5 Hz and then show a slight reduction beyond this point.

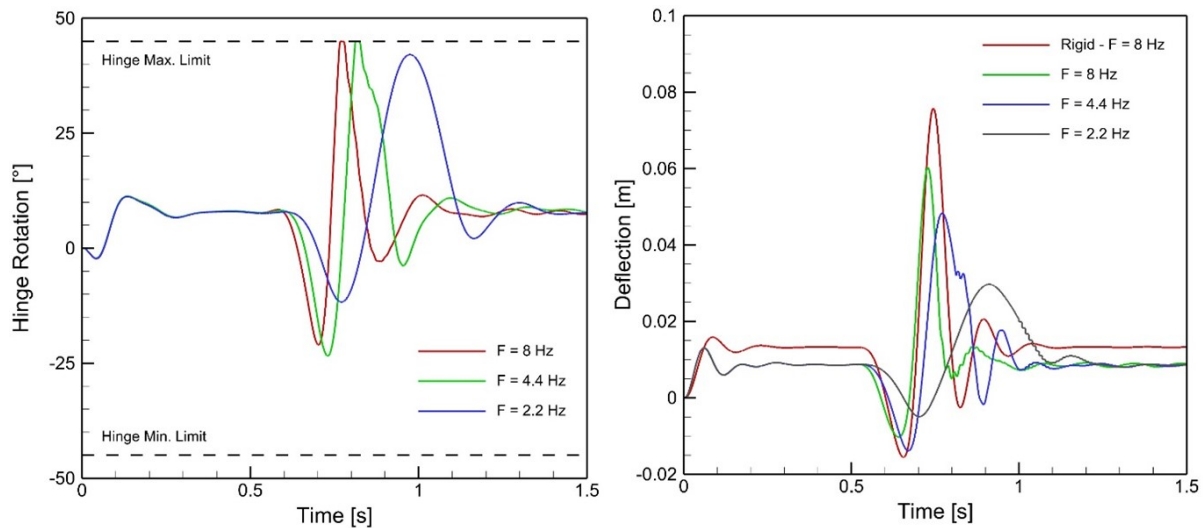


Figure 6: Hinge rotation response and Deflection of tip section of base wing subjected to a discrete gust with $W_g=0.2$ at gust frequencies $F=2.2$ Hz, 4.4 Hz, 8.0 Hz

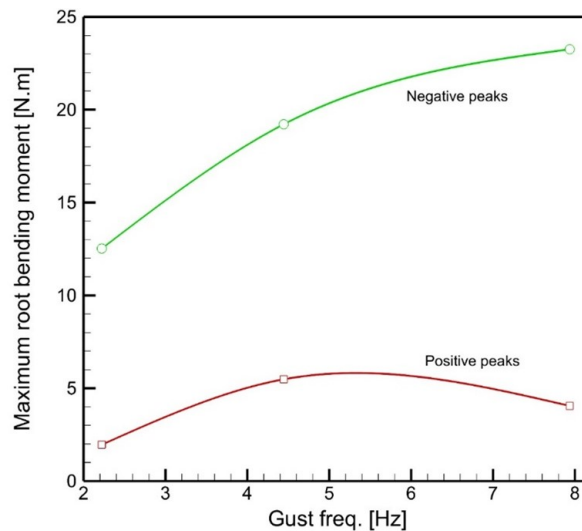


Figure 7: Comparison of peak positive and negative values at different gust frequencies

REFERENCES

- [1] E. Nakagawa, N. Tsushima, T. Aoki, T. Yokozeki, Sensitivity analysis and optimization of high-aspect-ratio wings with respect to mass and stiffness distributions, *Aerospace* 12 (12) (2025) 1090.
- [2] J. Xiong, S. Peng, J. Ren, L. Shen, Fluid–structure interactions of a high-aspect-ratio flexible wing in steady and unsteady flows, *Physics of Fluids* 37 (6) (2025).
- [3] F. Fernandez, D. Cleaver, I. Gursul, [Unsteady aerodynamics of flexible wings in transverse gusts](https://doi.org/10.1016/j.jfluidstructs.2021.103425), *Journal of Fluids and Structures* 108 (2022) 103425. doi:<https://doi.org/10.1016/j.jfluidstructs.2021.103425>. URL <https://www.sciencedirect.com/science/article/pii/S0889974621002024>
- [4] R. C. Cheung, D. Rezgui, J. E. Cooper, T. Wilson, Testing of folding wingtip for gust load alleviation of flexible high-aspect-ratio wing, *Journal of Aircraft* 57 (5) (2020) 876–888.
- [5] J. D. Ellis, D. Balatti, H. H. Khodaparast, S. Jiffri, M. I. Friswell, Active hinged wingtip control for reducing wing root bending moment, *Journal of Aircraft* (2025) 1–10.
- [6] S. Zhang, Y. Qiu, J. Sun, B. Wang, Z. Gao, Gust load alleviation control strategies for large civil aircraft through wing camber technology, in: *Actuators*, Vol. 13, MDPI, 2024, p. 229.
- [7] D. Balatti, H. Haddad Khodaparast, M. I. Friswell, M. Manolesos, M. Amoozgar, The effect of folding

- wingtips on the worst-case gust loads of a simplified aircraft model, *Proceedings of the Institution of Mechanical Engineers, Part G: Journal of Aerospace Engineering* 236 (2) (2022) 219–237.
- [8] M. Ahmadi, T. Farsadi, H. H. Khodaparast, Enhancing gust load alleviation performance in an optimized composite wing using passive wingtip devices: Folding and twist approaches, *Aerospace Science and Technology* 147 (2024) 109023.
 - [9] A. Castrichini, V. Hodigere Siddaramaiah, D. Calderon, J. E. Cooper, T. Wilson, Y. Lemmens, Nonlinear folding wing tips for gust loads alleviation, *Journal of Aircraft* 53 (5) (2016) 1391–1399.
 - [10] A. Molz, C. Breitsamter, Nonlinear Folding Wing Tips for Gust Loads Alleviation, *Deutsche Gesellschaft für Luft-und Raumfahrt-Lilienthal-Oberth eV*, 2024.
 - [11] R. M. Ajaj, E. I. Saavedra Flores, M. Amoozgar, J. E. Cooper, A parametric study on the aeroelasticity of flared hinge folding wingtips, *Aerospace* 8 (8) (2021) 221.
 - [12] D. Balatti, H. H. Khodaparast, M. I. Friswell, M. Manolesos, A. Castrichini, Experimental and numerical investigation of an aircraft wing with hinged wingtip for gust load alleviation, *Journal of Fluids and Structures* 119 (2023) 103892.